

Supplemental Materials

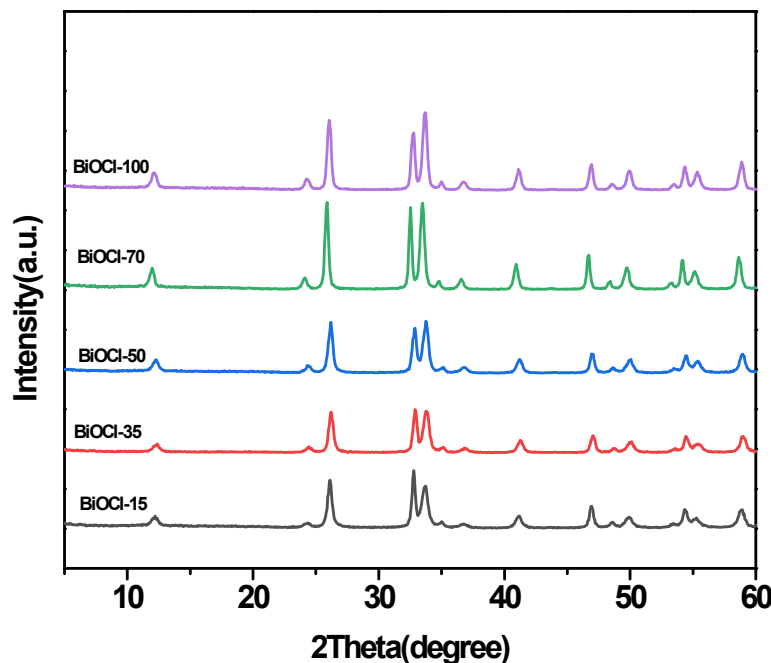


Fig. S1. XRD pattern of BiOCl prepared with existence of H3BTC.

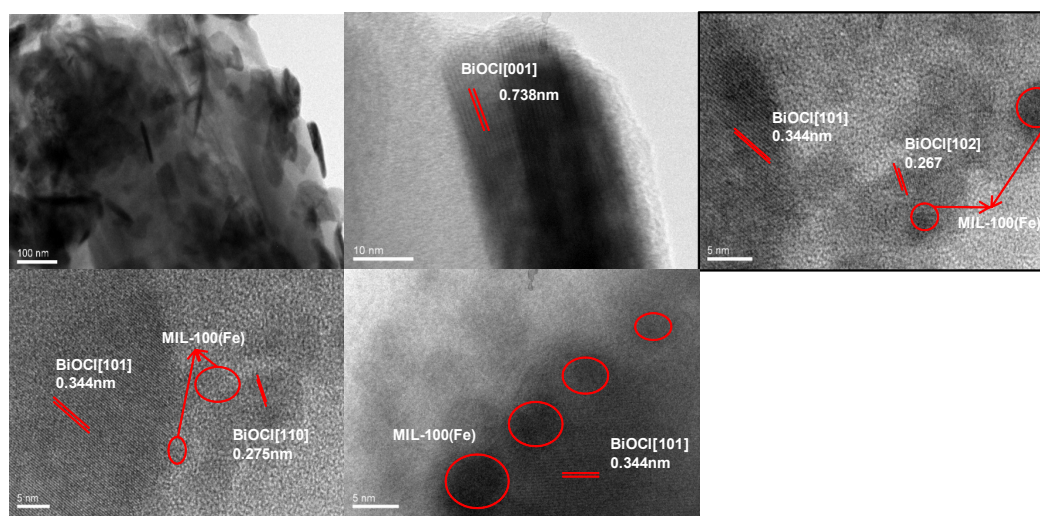


Fig. S2. TEM image of BMF-50.

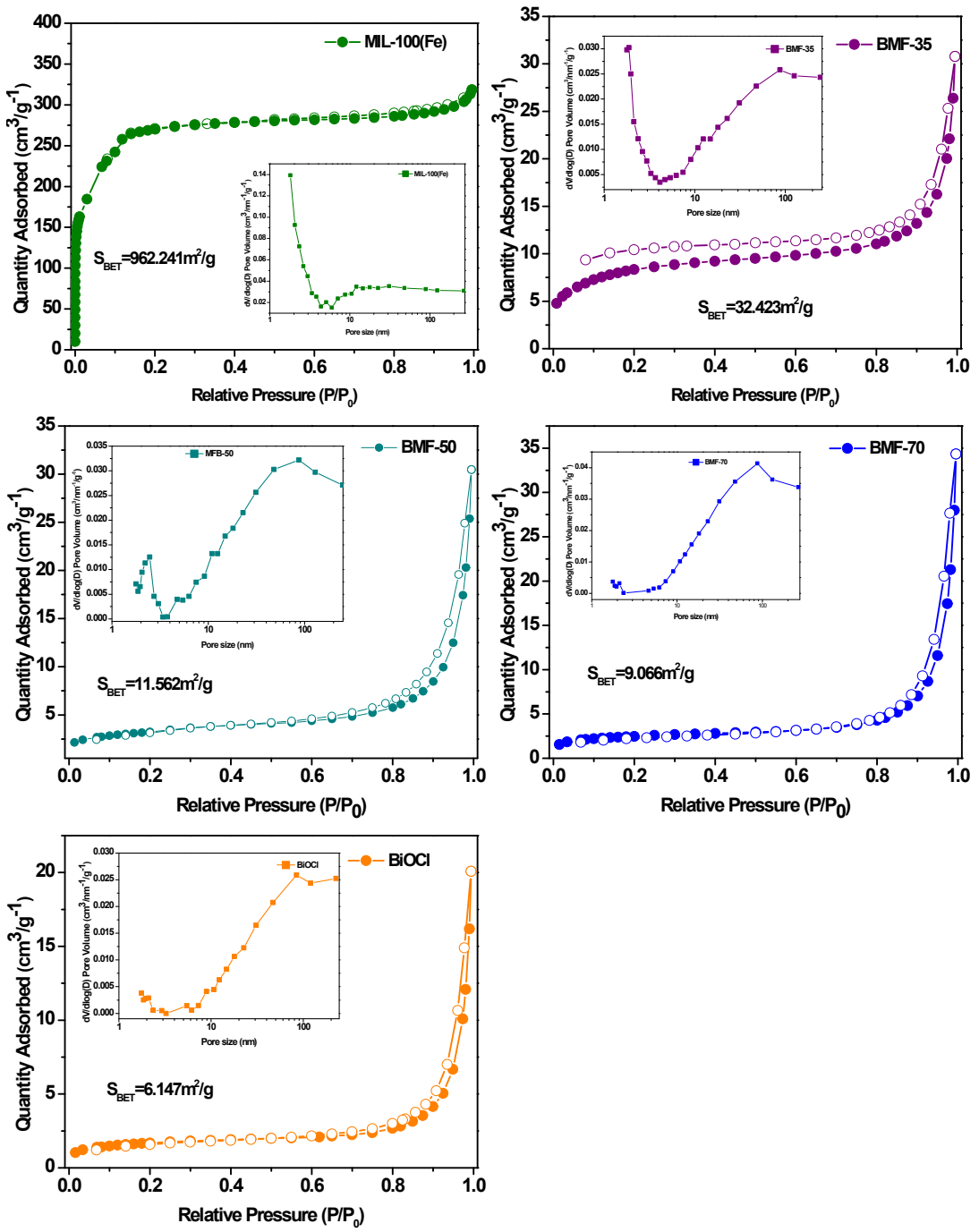


Fig. S3. Nitrogen adsorption-desorption isotherm and the pore size distribution curves for MIL-100(Fe), BMF-35, BMF-50, BMF-70, and BiOCl.

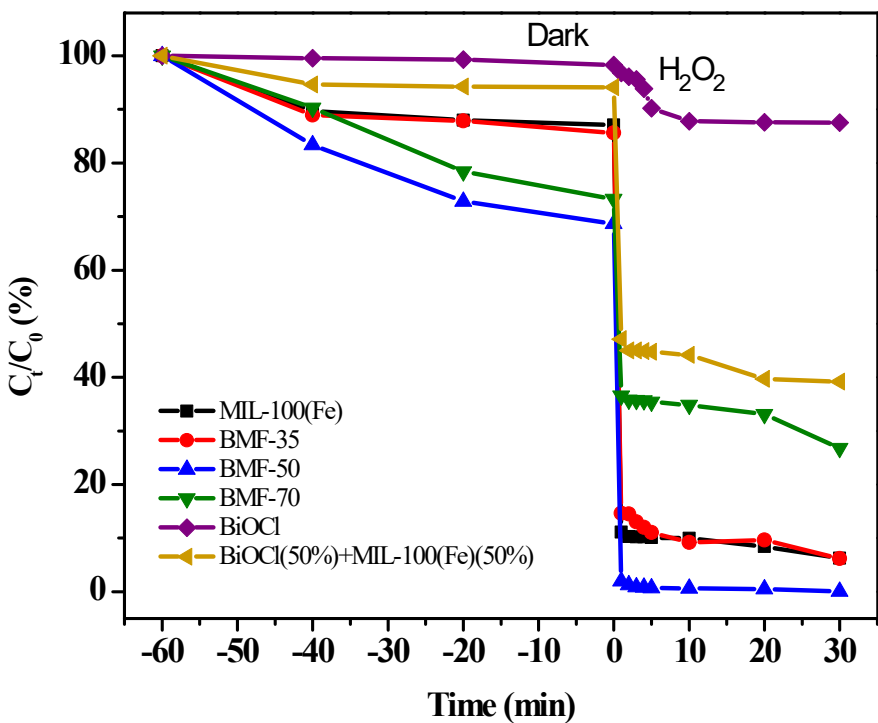


Fig. S4. The adsorption and degradation curves of MB using pure MIL-100(Fe), BiOCl, and BiOCl/MIL-100(Fe) hybrid materials as catalysts. ($T = 30^\circ\text{C}$, $[\text{H}_2\text{O}_2]_0 = 7.4 \text{ mmol/L}$, [catalyst] = 600 mg/L, $[\text{Dye}]_0 = 500 \text{ mg/L}$, pH=4.0)

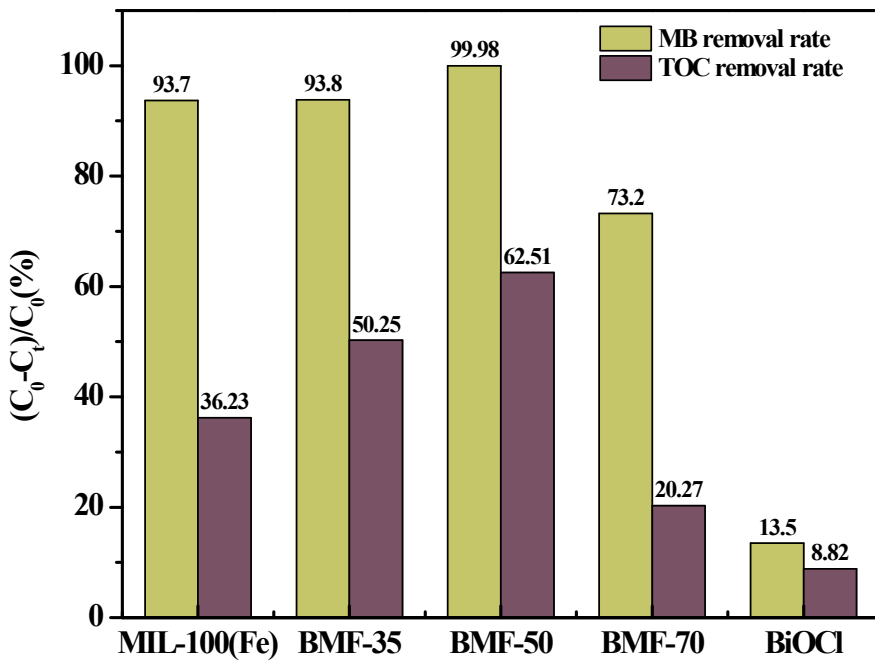


Fig. S5. TOC removal rate of MB with different catalysts after reacting for 30 min.

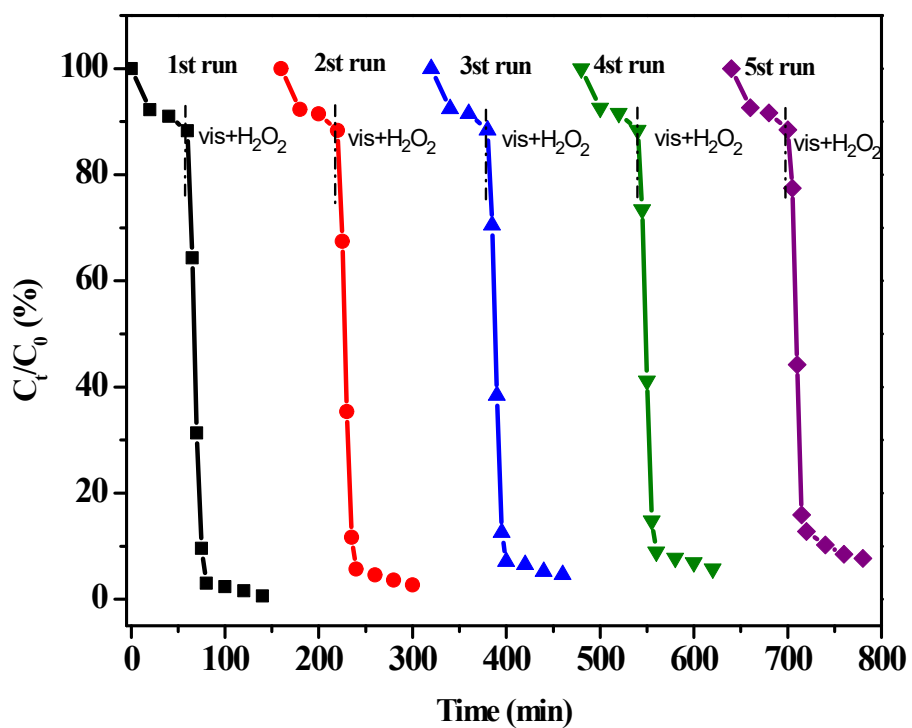


Fig. S6. Reusability of BMF-50 catalyst under the same conditions ($T = 30^\circ\text{C}$, $(\text{H}_2\text{O}_2)_0 = 7.44 \text{ mmol/L}$, (catalyst) = 80 mg/L, $[\text{RhB}]_0 = 40 \text{ mg/L}$)

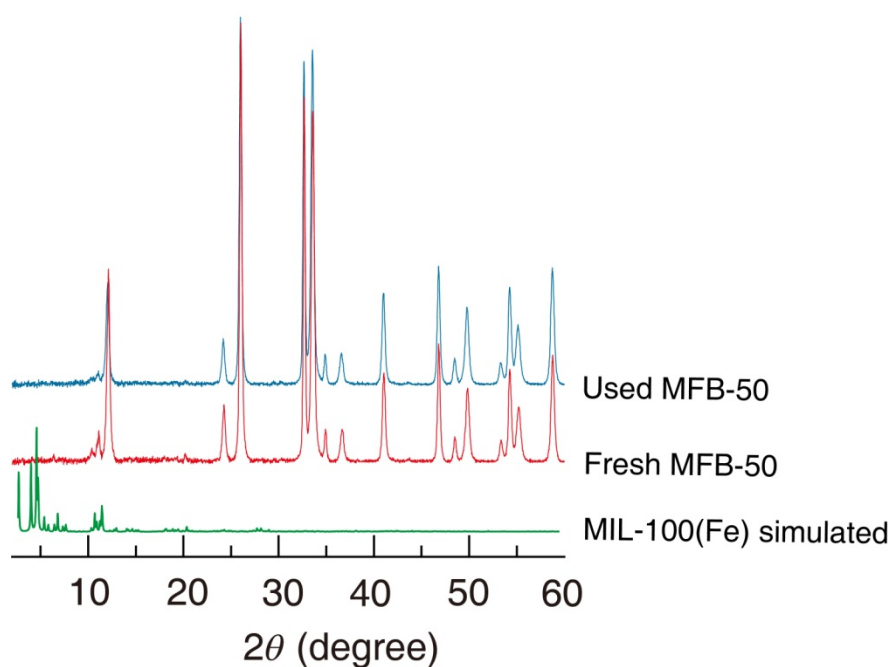


Fig. S7. XRD pattern of BMF-50 (fresh, used).

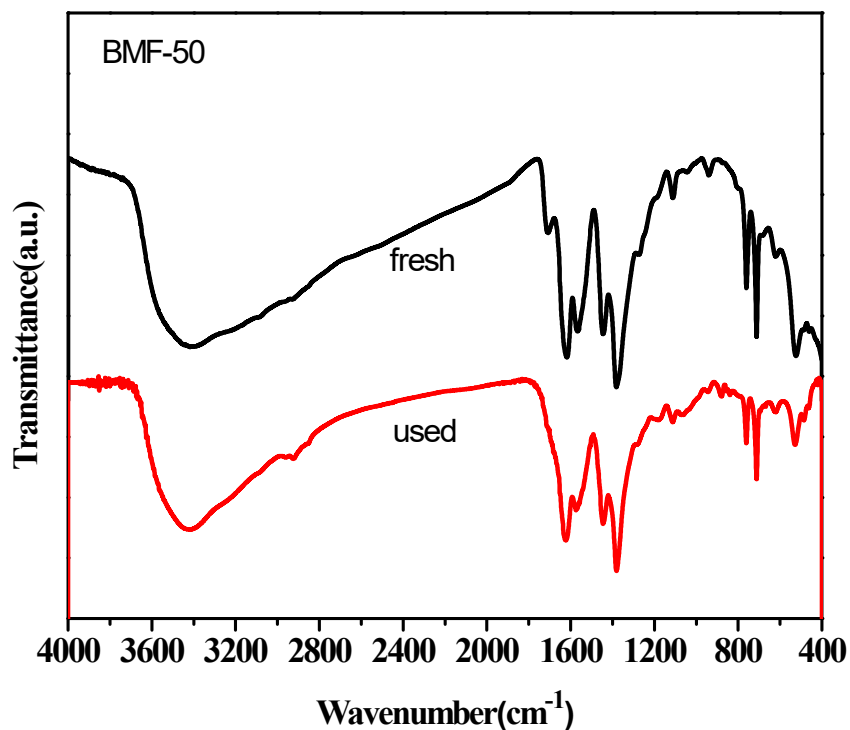


Fig. S8. FT-IR spectra of BMF-50 (fresh, used).

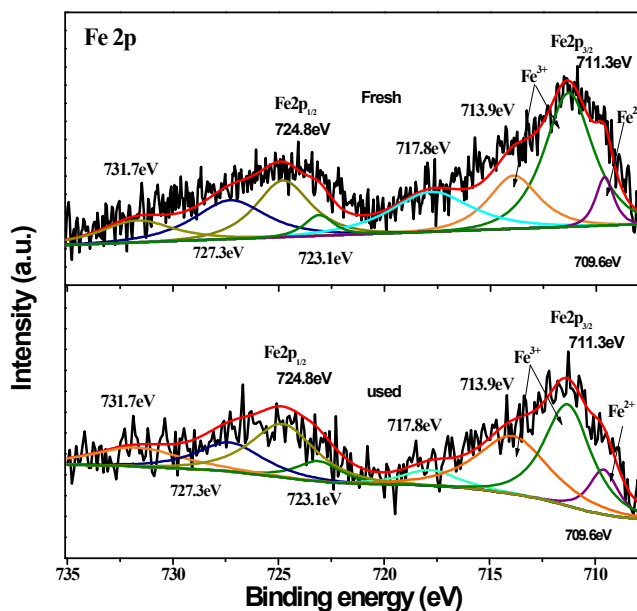


Fig. S9. Fe 2p XPS spectra of BMF-50 (fresh and used).

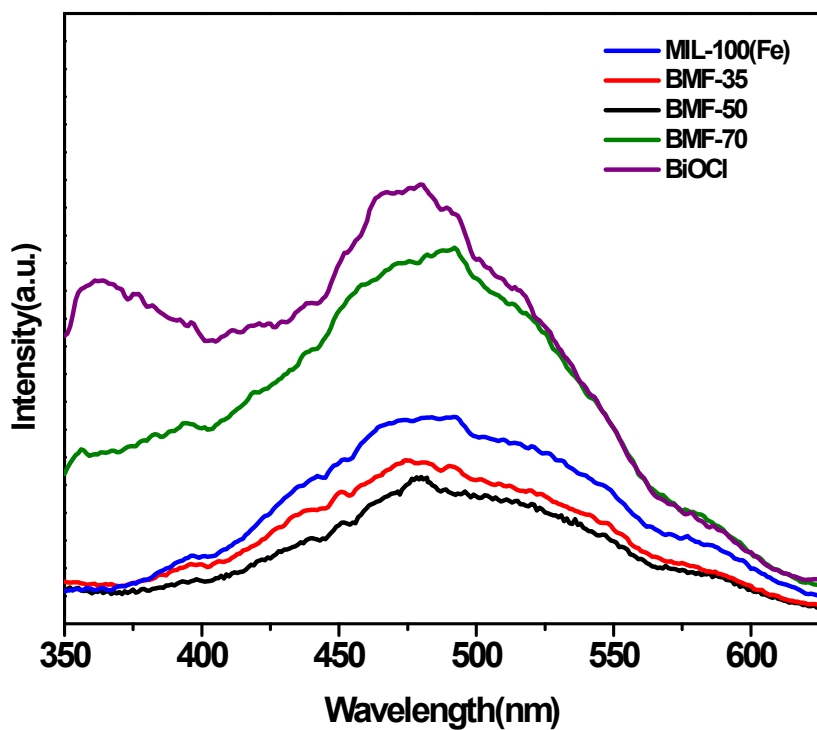


Fig. S10. PL spectra of the different composites.

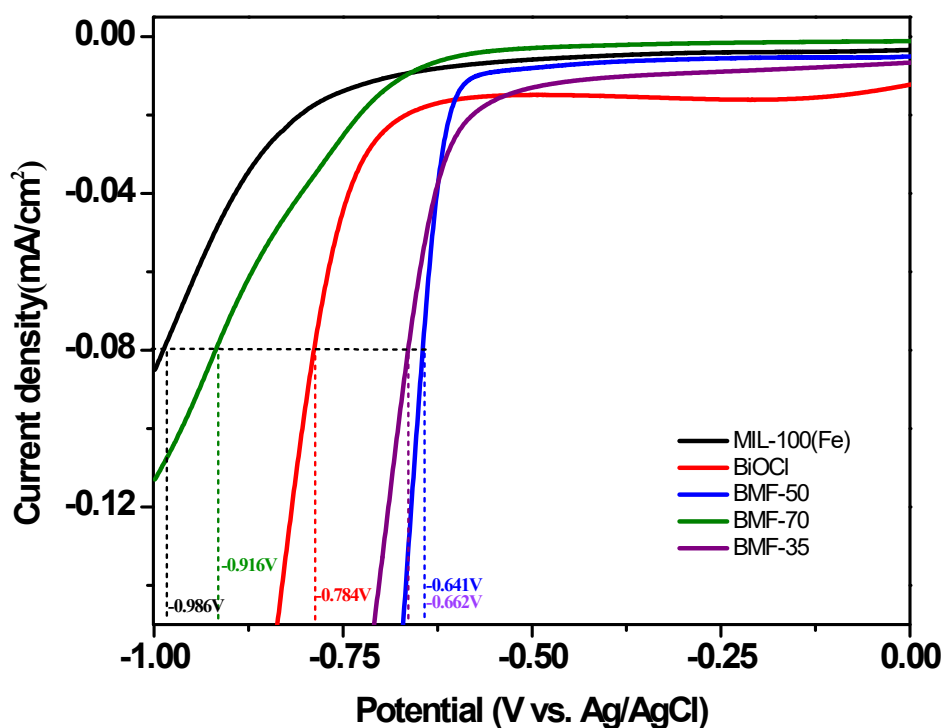


Fig. S11. LSV curves and onset potential of the samples to achieve the current density of $-0.08 \text{ mA}/\text{cm}^2$.

Table S1. The types and contents of BMF-(35,50,70) surface acids at different temperatures determined by Py -FTIR spectroscopy.

Sample	50°C		150°C		250°C	
	B	L	B	L	B	L
BMF-35	0.01623	0.06685	0.01362	0.05057	0.00579	0.02828
BMF-50	0.01747	0.04628	0.01725	0.03000	0.01203	0.02314
BMF-70	0.01668	0.01800	0.01339	0.00686	0.01021	0.00343

Unit: mmol/g

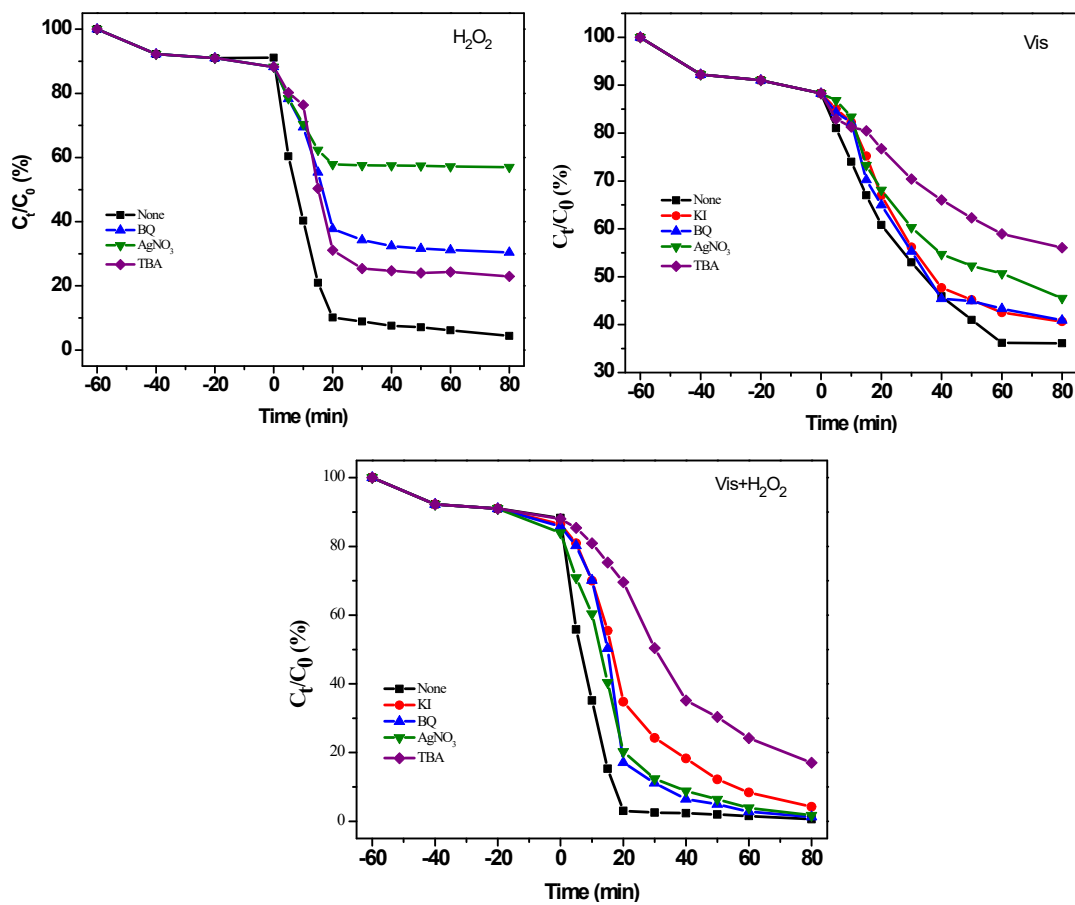


Fig. S12. RhB degradations by BMF-50 under visible light irradiation and H_2O_2 in the presence of several scavenger.

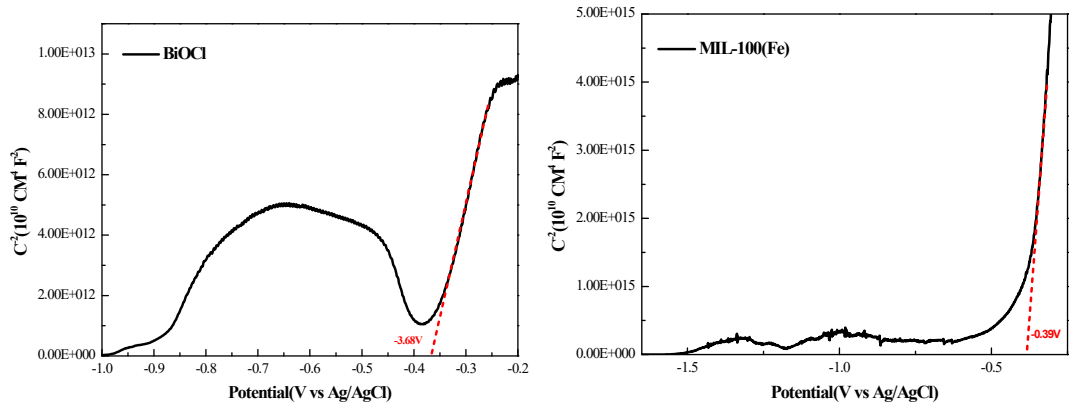


Fig. S13. Motschottky diagrams of MIL-100(Fe) and BiOCl.